Analytical description of the propagation of spatiotemporal solitons in fibers

Sergey V. Sazonov[*]

National Research Centre "Kurchatov Institute," 1 Kurchatova Square, Moscow 123182, Russia
and Lomonosov Moscow State University, 1 Leninskie Gory Street, Moscow 119991, Russia

(Received 24 June 2019; published 21 October 2019)

On the basis of the approximate method of the averaged Lagrangian, the propagation modes of spatiotemporal solitons in a graded-index optical fiber with a Kerr nonlinearity and anisotropic transverse distribution of the linear refractive index are investigated. It is shown that within the framework of the proposed approach, the equations for soliton parameters are formally similar to the dynamical equations of a two-dimensional quantum Bose liquid in an external field. Various modes of propagation in the form of light bullets localized in all directions were investigated. The conditions under which "dancing" light bullets can form are revealed. The trajectories of such objects are spatial Lissajous figures, turning into helical lines in the case of axially symmetric optical fibers. The fundamental spatiotemporal soliton is a special case of dancing light bullets. Under conditions when the diffraction spreading scale length is much shorter than the dispersion scale length, the transverse dynamics of a soliton does not depend on its longitudinal dynamics. In this case, the principal possibility of forming a wide class of light bullets with different transverse structures is shown. In addition, under these conditions, the spatiotemporal soliton mode of the self-imaging effect is described.

DOI: 10.1103/PhysRevA.100.043828

I. INTRODUCTION

The modern science about optical solitons originates from the invention of quantum generators of the visible frequency range, i.e., from the 1960s. There are spatial, temporal, and spatiotemporal solitons.

Spatial solitons are continuous beams, infinitely extended in the direction of propagation and localized in transverse directions. Focusing nonlinearity tends to compress the beam in transverse directions. This process can be prevented by diffraction. The mutual compensation of these effects is capable of forming the spatial soliton.

Temporal solitons are pulses of finite temporal duration and infinitely extended in transverse directions. Here the nonlinear temporal self-compression of the pulse is compensated by dispersive spreading.

Spatiotemporal solitons (light bullets) can be considered as a symbiosis of spatial and temporal solitons. Light bullets are bunches of light energy, localized in all directions. According to the above, focusing nonlinearity, dispersion, and diffraction take part in the formation of light bullets. Let us note that these three physical effects are necessary, but not sufficient for the formation of light bullets. It is well known, for example, that the focusing Kerr (cubic) nonlinearity, combined with anomalous group velocity dispersion (DGV) and diffraction, is not able to form a light bullet in a homogeneous bulk medium [1]. It requires the presence of other types of nonlinearity: saturating, Raman, etc. [1].

Another opportunity for the formation of a spatiotemporal soliton can be provided by linear refraction in an inhomogeneous medium. The role of such medium can performed a fiber light guide. For example, in a graded-index fiber, the refractive index continuously changes from its center to the periphery. Thus, in the general case, the formation of a light bullet requires the presence of nonlinearity, dispersion, diffraction, and of spatial inhomogeneity of the medium.

In fibers with anomalous DGV, bright solitons can be formed. In the case of normal DGV, dark solitons are formed under certain conditions. We note that both bright and dark solitons in optical fibers were observed experimentally. In [2], bright dissipative solitons were observed. Dark solitons in the form of vector domain polarization walls in a fiber ring laser were also observed [3]. We also note the experimental observation of dark and bright solitons in the spectral range with both normal and anomalous DGV [4].

It should be noted that theoretical studies devoted to the propagation of optical solitons in optical fibers are based on numerical simulations [5]. At the same time, satisfactory analytical approaches have not been developed. There is a simple approximate approach associated with the factorized dependence of the envelope of the light field on time and transverse coordinates [6]. However, this approach does not answer the question about the stability of light bullets and the conditions for their formation. We note in this regard that light bullets can be used in fiber-optic communication systems. Therefore, analytical studies of the formation and propagation of light bullets in optical fibers are highly desirable and relevant.

This paper proposes a description of the waveguide propagation of spatiotemporal solitons based on the development of the method of an averaged Lagrangian applied to the transversely inhomogeneous media. This method has proven itself in the theory of temporal and spatiotemporal solitons propagating in homogeneous bulk media [7–13].

[*]sazonov.sergey@gmail.com

The paper is organized as follows. Section II gives a nonlinear wave equation for the complex envelope of the electric field of a light pulse. This equation is a nonlinear Schrödinger equation (NLS), supplemented by a term that takes into account the spatial inhomogeneity of the refractive index. In this section is described the scheme of the averaged Lagrangian method based on a trial solution in the form of a spatiotemporal soliton. It is shown that the equations for the parameters of this soliton are formally similar to the hydrodynamic equations for a quantum Bose liquid, which can be transformed into a modified Gross-Pitaevskii equation. In Sec. III, the solutions of these equations are found in the form of a "dancing" light bullet and a fundamental spatiotemporal soliton. Section IV is devoted to a brief analysis of solutions of the type of light bullets in the approximation of the diffraction limit. In this limit, the transverse diffraction spreading of a light pulse occurs much faster than spreading along the direction of propagation. As an example, the soliton version of the self-imaging effect resulting from the interference of various soliton modes of a fiber is considered here. In Sec. V, the general conclusions are formulated; the advantages and disadvantages of the proposed analytical approach are noted.

II. AVERAGED LAGRANGIAN APPROACH. SOLUTIONS FOR SOLITON PARAMETERS

For a pulse propagating in a transversely inhomogeneous nonresonant medium with a Kerr nonlinearity, the following equation is true [1,14,15]:

$$i\frac{\partial\psi}{\partial z} = -\frac{\beta_2}{2}\frac{\partial^2\psi}{\partial\tau^2} + \alpha|\psi|^2\psi + g(\mathbf{r})\psi + \frac{c}{2n_0\omega}\Delta_\perp\psi. \quad (1)$$

Here ψ is the envelope of the electric field E of the pulse $E = \psi\exp[i(\omega t - kz)] + \text{c.c.}$; ω and k are the carrier frequency and wave number, respectively; z is the coordinate along the direction of a pulse propagation (longitudinal coordinate); $\tau = t - z/v_g$ is the "local" time, v_g is the linear group velocity on the central axis of the fiber; $\beta_2 = \frac{\partial}{\partial\omega}(\frac{1}{v_g})$ is the DGV parameter; c is the speed of light in a vacuum; $n_0 = \sqrt{1+4\pi\chi_0}$ and χ_0 are the linear refractive index and linear susceptibility on the central axis of fiber, respectively; the coefficient $g(\mathbf{r})$ determines the linear refraction of the matter of the fiber:

$$g(\mathbf{r}) = \frac{\omega}{c}\frac{n_0^2-1}{2n_0}f(\mathbf{r}). \quad (2)$$

$\mathbf{r}$ is the transversal radius vector, $f(\mathbf{r})$ is the dimensionless function characterizing the transverse distribution of the linear dielectric susceptibility of the medium: $\chi(\mathbf{r}) = \chi_0[1+f(\mathbf{r})]$, $f(0)=0$; $\Delta_\perp$ is the transversal Laplacian; α is the coefficient of the Kerr nonlinearity which is determined by the expression

$$\alpha = \frac{\omega}{2\pi n_0}n_2, \quad (3)$$

where n_2 is the nonlinear refractive index determined through the refractive index n depending on the pulse intensity I: $n = n_0 + n_2 I$.

In the case of a focusing fiber, the function $f(\mathbf{r})$ decreases from the center of the waveguide to its periphery. In the defocusing case, the situation is opposite.

Under the condition $\alpha > 0$ ($\alpha < 0$) the Kerr nonlinearity is focusing (defocusing).

Equation (1) corresponds to the Lagrangian density:

$$L = \frac{i}{2}\left(\psi^*\frac{\partial\psi}{\partial z} - \psi\frac{\partial\psi^*}{\partial z}\right) - g|\psi|^2 - \frac{\beta_2}{2}\left|\frac{\partial\psi}{\partial\tau}\right|^2 - \frac{\alpha}{2}|\psi|^4 + \frac{c}{2n_0\omega}|\nabla_\perp\psi|^2. \quad (4)$$

The mathematical procedure used in this section originates from Refs. [9–13]. In these papers, the influence of transverse perturbations on the temporal solitons in homogeneous bulk media was considered. Applied to our case, this corresponds to the identity $g(\mathbf{r}) = 0$ in Eq. (1). Here we consider the generalization of this method to the case when $g(\mathbf{r}) \neq 0$.

First we put $g(\mathbf{r}_\perp) = \Delta_\perp\psi = 0$ in Eq. (1). In this case, Eq. (1) has a solution in the form of a temporal soliton,

$$\psi = \frac{1}{\tau_p}\sqrt{-\frac{\beta_2}{\alpha}}\exp\left(i\frac{\beta_2 z}{2\tau_p^2}\right)\operatorname{sech}\left(\frac{\tau}{\tau_p}\right), \quad (5)$$

where τ_p is the free parameter that has the meaning of the temporal pulse duration.

Accounting for the last two terms on the right-hand side of (1) being carried out, we choose a trial solution on the basis of temporal soliton (5). However, we now assume that the parameter τ_p is an unknown function of the coordinates. We make the same assumption regarding the imaginary exponent in (5). Thus, we choose a trial solution in the form

$$\psi = \sqrt{-\frac{\beta_2}{\alpha}}e^{i\theta}\rho\operatorname{sech}(\rho\tau), \quad (6)$$

where ρ and θ are the unknown functions of the coordinates z and $\mathbf{r}$.

Substituting (6) into (4) and integrating the resulting expression on τ, we arrive at the averaged Lagrangian Λ. Ignoring the nonessential constant factor, we have

$$\Lambda = \int_{-\infty}^{+\infty} L d\tau \sim -\frac{c}{n_0\omega}\rho\frac{\partial\theta}{\partial z} + \frac{c\beta_2}{6n_0\omega}\rho^3 + \left(\frac{c}{n_0\omega}\right)^2 \times\left[\rho\frac{(\nabla_\perp\theta)^2}{2} + \frac{1}{6}\left(\frac{\pi^2}{12}+1\right)\frac{(\nabla_\perp\rho)^2}{\rho}\right] - \frac{c}{n_0\omega}g\rho. \quad (7)$$

Now, using (7), we write the Euler-Lagrange equations with respect to variables ρ and θ:

$$\frac{\partial}{\partial z}\frac{\partial\Lambda}{\partial(\partial\theta/\partial z)} + \nabla_\perp\frac{\partial\Lambda}{\partial(\nabla_\perp\theta)} = 0, \quad \frac{\partial\Lambda}{\partial\rho} - \nabla_\perp\frac{\partial\Lambda}{\partial(\nabla_\perp\rho)} = 0.$$

As a result, we obtain the set of equations

$$\frac{\partial\rho}{\partial z} + \nabla_\perp(\rho\nabla_\perp\varphi) = 0, \quad (8)$$

$$\frac{\partial\varphi}{\partial z} + \frac{(\nabla_\perp\varphi)^2}{2} + \frac{c\beta_2}{2n_0\omega}\rho^2 - \frac{c}{n_0\omega}g(\mathbf{r}) = \frac{\mu^2}{2}\left(\frac{c}{n_0\omega}\right)^2\frac{\Delta_\perp\sqrt{\rho}}{\sqrt{\rho}}. \quad (9)$$

Here

$$\varphi = -\frac{c}{n_0\omega}\theta, \quad \mu = 2\sqrt{\frac{1}{3}\left(\frac{\pi^2}{12}+1\right)} \approx 1.559. \quad (10)$$

The right-hand side of (9) takes into account diffraction effects. The system (8) and (9) is identical to the equations for a quantum Bose liquid in an external field [16]. The right-hand side of (9) is sometimes called quantum pressure. Neglecting this term corresponds to the approximation of geometrical optics. In this case, the system (8) and (9) is identical to the set of equations for the two-dimensional flow of an ideal fluid [17,18]. The coordinate z here performs the role of time, and the dynamic variables ρ and φ act as the density of the fluid and the potential of the velocity field, respectively. The third term on the left-hand side of (9) corresponds to the internal pressure of an imaginary fluid. The last term on the left-hand side of this equation corresponds to the density of the potential energy of the external field in which the fluid is placed. This term takes into account the dependence of the refractive index of the fiber on the transverse coordinate.

We introduce the complex function associated with the variables ρ and φ by Madelung transformation [1,13,19,20]:

$$\Phi = \sqrt{\rho}\exp\left(i\frac{n_0\omega}{c\mu}\varphi\right) = \sqrt{\rho}\exp\left(-i\frac{\theta}{\mu}\right). \qquad (11)$$

It is easy to see that the system (8) and (9) is equivalent to the equation

$$i\frac{\partial\Phi}{\partial z} = -\frac{\mu c}{2n_0\omega}\Delta_\perp\Phi + \frac{\beta_2}{2\mu}|\Phi|^4\Phi - \frac{g(\mathbf{r})}{\mu}\Phi. \qquad (12)$$

Taking into account the above, Eq. (12) can be called the modified Gross-Pitaevskii equation for a two-dimensional Bose-Einstein condensate in an external field. The modification here is due to the fact that the Gross-Pitaevskii equation contains cubic nonlinearity [21]. At the same time, the degree of nonlinearity of Eq. (12) is 5. The external field is taken into account by the last term on the right-hand side of Eq. (12).

On the other hand, Eq. (12) describes the propagation of an optical beam in a fiber with a fifth-degree nonlinearity. Therefore, it can be said that the procedure used in this section reduces Eq. (1) for the propagation of a pulse in a fiber with a cubic nonlinearity to Eq. (12) for a certain beam propagating in a fiber with a fifth-degree nonlinearity.

One can find various solutions of Eq. (12) [or of system (8) and (9)] and thus analyze the behavior of the functions ρ and φ. As a result, the dynamics of the optical pulse in the fiber will be studied.

III. DANCING LIGHT BULLET AND FUNDAMENTAL SPATIOTEMPORAL SOLITON

We assume below that the linear susceptibility has a parabolic profile in the cross section of a fiber: $\chi(\mathbf{r}) = \chi_0[1-(\frac{x^2}{a_x^2}+\frac{y^2}{a_y^2})]$. When

$$f(\mathbf{r}) = f(x,y) = -\left(\frac{x^2}{a_x^2}+\frac{y^2}{a_y^2}\right),\quad g(\mathbf{r}) = -\frac{\omega}{2c}\left(\varepsilon_x^2x^2+\varepsilon_y^2y^2\right), \qquad (13)$$

where a_x and a_y are the constants characterizing the transverse scales of the fiber along the x and y axes respectively,

$$\varepsilon_j = \frac{\sqrt{n_0^2-1}}{n_0 a_j}. \qquad (14)$$

Here and everywhere below $j = x, y$.

When $a_{x,y}^2 > 0$ ($a_{x,y}^2 < 0$) the fiber is focusing (defocusing). Generally speaking, we assume that the fiber does not have axial symmetry; i.e. $a_x \neq a_y$.

Let us determine also the dispersion scale length l_d and the diffraction scale lengths l_{Dj} by the expressions

$$l_d = \frac{2\tau_p^2}{|\beta_2|},\quad l_{Dj} = \frac{n_0\omega}{c}R_{j0}^2 = 2\pi n_0\frac{R_{j0}^2}{\lambda}, \qquad (15)$$

where $\lambda = 2\pi c/\omega$ is the wavelength corresponding to the carrier frequency ω, R_{x0} and R_{y0} are the equilibrium scale lengths (apertures) of this soliton along the x axis and y axis, respectively (see below).

When finding solutions to system (8) and (9), we use the Cartesian coordinate system.

Equations (A14) and (A15) in the Appendix for the soliton apertures R_x and R_y are similar to the system of equations for the motion of two Newtonian particles of unit mass in a field with the "potential energy" (A15). The interaction between these particles is described by the last term on the right-hand side of (A15).

The function $U(R_x, R_y)$ is a surface in the space of variables R_x and R_y. The stationary solutions of Eq. (A15) correspond to the local minimum of the function $U(R_x, R_y)$ under conditions $R_x = R_{x0}$ and $R_y = R_{y0}$. We write the conditions for the existence of the extremum in the form

$$\left(\frac{\partial U}{\partial R_x}\right)_0 = \left(\frac{\partial U}{\partial R_y}\right)_0 = 0.$$

Hereinafter, the subscript "0" corresponds to the fact that $R_x = R_{x0}$ and $R_y = R_{y0}$.

From here and from (A15), with accounting for (15), we obtain

$$\varepsilon_j^2 = \frac{\mu^2}{4l_{Dj}^2} + \frac{2\mathrm{sgn}(\beta_2)}{l_d l_{Dj}}. \qquad (16)$$

From (16), (A1)–(A5), (A12), (A17), (A10), and the first expression in (10), taking into account that $R_j = R_{j0} = \text{const.}$, we find

$$\theta = \left[\frac{\mu^2}{4}\sum_{j=x,y}\frac{1}{l_{Dj}} + \frac{\mathrm{sgn}(\beta_2)}{l_d}\right]z + \frac{n_0\omega}{c} \times \sum_{j=x,y}\varepsilon_j q_{j0}\left\{\frac{q_{j0}}{4}\sin[2(\varepsilon_j z+\delta_j)] + x_j\cos(\varepsilon_j z+\delta_j)\right\}, \qquad (17)$$

$$\rho = \frac{1}{\tau_p}\exp\left\{-\sum_{j=x,y}\frac{[x_j - q_{j0}\sin(\varepsilon_j z+\delta_j)]^2}{2R_{j0}^2}\right\}. \qquad (18)$$

It is believed here that $x_x = x$, $x_y = y$.

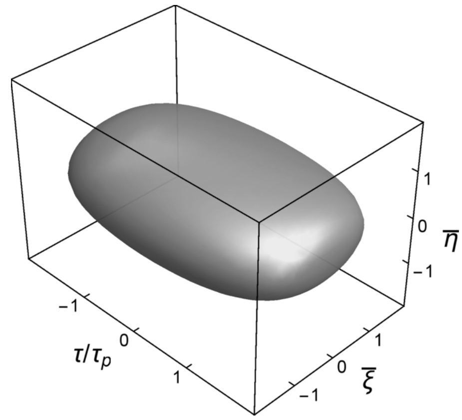

FIG. 1. Schematic representation of a constant-intensity surface of the dancing light bullet in the traveling framework under the condition $a_x = 2a_y$; $\bar{\xi}$ and $\bar{\eta}$ are the dimensionless variables, determined by the relations $\bar{\xi} = (x - q_x)/R_{y0}$ and $\bar{\eta} = (y - q_y)/R_{y0}$, respectively.

Figure 1 schematically displays the surface of constant intensity $\sim|\psi|^2 \sim \rho^2 \text{sech}^2[\rho(t - z/v_g)]$ of the spatiotemporal soliton (6), (18) in the optical fiber under the condition $a_x \neq a_y$. It is clear that such soliton is not axially symmetric.

According to expressions (6) and (18), the center of a bunch of light energy $\sim|\psi|^2 \sim \rho^2 \text{sech}^2[\rho(t - z/v_g)]$ propagates along a trajectory described by the parametric equations (see Fig. 2):

$$z_c = v_g t, x_c = q_{x0} \sin(\omega_x t + \delta_x), \quad y_c = q_{y0} \sin(\omega_y t + \delta_y). \tag{19}$$

Here $\omega_j = v_g \varepsilon_j$.

In the transverse plane $z = v_g t$, the center of the light bullet describes the Lissajous figures. These figures are the superposition of oscillatory movements along the x and y axes with frequencies ω_1 and ω_2, respectively. The spatiotemporal soliton, which is displayed in Fig. 1, propagates along this trajectory.

The solution discussed can be called the dancing light bullet. This solution has five free parameters: δ_x, δ_y, q_{x0}, q_{y0}, and τ_p. The first four parameters define the Lissajous figure. Given the temporal duration τ_p, we use (16) and (15) to determine the components R_{j0} of the aperture of the light bullet. In addition, the amplitude of this light bullet is also uniquely determined by the temporal duration τ_p [see (6) and (18)].

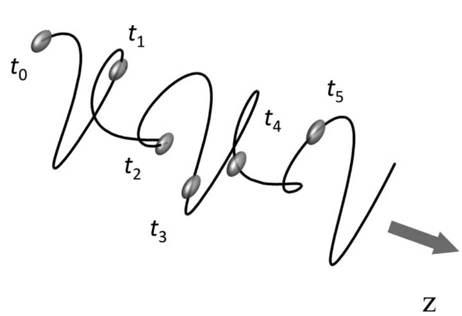

FIG. 2. Schematic representation of propagation trajectory of dancing light bullet in the fiber, defined by the expressions (19): $\omega_x/\omega_y = a_y/a_x = 1.5$, $\delta_2 = \delta_1 + \pi/2$. Designations $t_0 < t_1 < t_2 < t_3 < t_4 < t_5$ correspond to the different points in time t.

Putting $l_{Dj} \sim R_{j0}^2 \to \infty$, $\varepsilon_j \sim 1/a_j = 0$ into Eqs. (17) and (18), we come to the case of a one-dimensional (temporal) soliton in a homogeneous medium. In this case, it follows from (17) and (18) that $\theta = \frac{\text{sgn}(\beta_2)}{l_d} z = \frac{\beta_2 z}{2\tau_p^2}$, $\rho = \frac{1}{\tau_p}$ [see also (15)]. Equalities (16) turn into identities $0 = 0$. That is, the solution (6) and (16)–(18) exactly passes to the soliton (5). This circumstance is an important argument in favor of our approach.

The dancing light bullet which is described by the expressions (16)–(18) is stable, if the local extremum of a function $U(R_x, R_y)$ [see (A15)] is its minimum. This requires the implementation of inequalities $A_1 > 0$, $A_2 > 0$, and $A_1 A_2 - B^2 > 0$, where

$$A_j = \left(\frac{\partial^2 U}{\partial R_j^2}\right)_0 = \varepsilon_j^2 + \frac{3\mu^2}{4 l_{Dj}^2} + 6\frac{\text{sgn}(\beta_2)}{l_d l_{Dj}},$$

$$B = \left(\frac{\partial^2 U}{\partial R_x \partial R_y}\right)_0 = 4\frac{\text{sgn}(\beta_2)}{l_d \sqrt{l_{Dx} l_{Dy}}}.$$

It is easy to see from here that under the condition $\beta_2 > 0$ the inequality $A_1 A_2 - B^2 > 0$ is performed automatically. At the same time, as can be seen from (16), inequalities $A_1 > 0$ and $A_2 > 0$ are equivalent to the conditions

$$\varepsilon_j^2 > 0. \tag{20}$$

The conditions (20) can be carried out for the focusing fiber only, when $\varepsilon_x^2 > 0$ and $\varepsilon_y^2 > 0$. In the defocusing fiber ($\varepsilon_x^2 < 0$ or $\varepsilon_y^2 < 0$) or in the absence of a fiber ($A = 4\varepsilon_x^2 = B = 4\varepsilon_y^2 = 0$), a stable light bullet cannot form. The last conclusion agrees with the well-known statement for a homogeneous medium with Kerr nonlinearity [1].

In a focusing fiber with a normal DGV ($\beta_2 > 0$) within the framework of the physical model used, a stable light bullet can form without other conditions on the parameters of the optical pulse [see (16) and (20)]. Therefore, below we consider the case of anomalous DGV ($\beta_2 < 0$). It is this case that has an important applied significance [1].

From (6) and (3) it follows that a stable light bullet under the condition $\beta_2 < 0$ can form if $n_2 > 0$. That is, the Kerr nonlinearity must be focusing. Such a situation is realized in the fused silica fiber [1].

The equalities (16) allow us to exclude some parameters from the inequality $A_1 A_2 - B^2 > 0$. Excluding in series l_{Dj}, l_d, and ε_j, after simple mathematical transformations, we have

$$\frac{1}{\sqrt{1 + H_x}} + \frac{1}{\sqrt{1 + H_y}} < 1, \tag{21}$$

$$3G_x G_y + G_x + G_y > 1, \tag{22}$$

$$2(Q_x + Q_y) - 3Q_x Q_y < 1, \tag{23}$$

where $H_j = (\frac{\mu l_d \varepsilon_j}{2})^2$, $G_j = (\frac{2 l_{Dj} \varepsilon_j}{\mu})^2$, and $Q_j = \frac{4 l_{Dj}}{\mu^2 l_d}$.

Under conditions (20)–(23) in the case $\beta_2 < 0$ the approximate solution (6) and (16)–(18) of Eq. (1) is stable.

The meaning of conditions (21)–(23) is most transparent in the case when the fiber and the optical pulse are axially symmetric: $a_x = a_y = a$, $R_{x0} = R_{y0} = R_0$, $R_x = R_y = R$,

$$q_{x0} = q_{y0} = q_0,$$

$$\varepsilon_x = \varepsilon_y = \varepsilon = \frac{\sqrt{n_0^2 - 1}}{n_0 a}, \quad l_{Dx} = l_{Dy} = l_D = \frac{n_0\omega}{c} R_0^2 = 2\pi n_0 \frac{R_0^2}{\lambda}. \tag{24}$$

In this case, instead of the system (A14), for the soliton aperture R we have the equation

$$R'' = -\frac{\partial U}{\partial R}, \tag{25}$$

where the potential energy (A15) takes the form

$$U(R) = \frac{\varepsilon^2}{2} R^2 + \frac{\mu^2}{8}\left(\frac{c}{n_0\omega}\right)^2 \frac{1}{R^2} + \frac{c}{2n_0\omega} \frac{\mathrm{sgn}(\beta_2)}{l_d} \frac{R_0^4}{R^4}. \tag{26}$$

From (16) and (21)–(23) under conditions $H_x = H_y = H$, $G_x = G_y = G$, and $Q_x = Q_y = Q$ we have $H > 3$, $G > 1/3$, and $Q < 1/3$. Then, using the expressions for H, G, and Q, we write in the axially symmetric case

$$l_d^2 > \frac{12}{\mu^2\varepsilon^2}, \quad l_D^2 > \frac{\mu^2}{12\varepsilon^2}, \quad \frac{l_D}{l_d} < \frac{\mu^2}{12}. \tag{27}$$

Using (24), the first expression in (15), and the second expression in (10), we rewrite these inequalities in the following form:

$$R_0 > R_{\min} = 0.27 \frac{\sqrt{\lambda a}}{\left(n_0^2 - 1\right)^{1/4}}, \tag{28}$$

$$\tau_p > \tau_{\min} = 1.05 \frac{\sqrt{n_0|\beta_2| a}}{\left(n_0^2 - 1\right)^{1/4}}, \tag{29}$$

$$\frac{R_0}{\tau_p} < \frac{R_{\min}}{\tau_{\min}} = 0.25\sqrt{\frac{\lambda}{n_0|\beta_2|}}. \tag{30}$$

The above Lissajous figures here are ellipses. Assuming, moreover, in (17) and (18) $\delta_x - \delta_y = \pi/2$, we obtain

$$\theta = \left[\frac{\mu^2}{2l_D} + \frac{\mathrm{sgn}(\beta_2)}{l_d}\right] z + \frac{n_0\omega}{c} \varepsilon \mathbf{r}_c \cdot \mathbf{r}, \tag{31}$$

$$\rho = \frac{1}{\tau_p} \exp\left(-\frac{|\mathbf{r} - \mathbf{r}_c|^2}{2R_0^2}\right), \tag{32}$$

where $\mathbf{r}_c$ is the transverse radius-vector of the soliton center, defined in the polar coordinate system (r_c, φ_c) by the expressions

$$r_c = q_0, \quad \varphi_c = \varepsilon z_c + \delta_y \tag{33}$$

[see (19) under conditions $q_{x0} = q_{y0} = q_0$, $\varepsilon_x = \varepsilon_y = \varepsilon$, and $\delta_x = \delta_y + \pi/2$].

Here, Lissajous figures take the form of circles with the radius q_0. In this case, the center of the soliton moves along a helical spatial line with a pitch

$$h = \frac{2\pi}{\varepsilon} = \frac{2\pi n_0 a}{\sqrt{n_0^2 - 1}}.$$

The surfaces of constant intensity of the soliton (6), (31), and (32), corresponding to different time points, are schematically shown in Fig. 3. This axially symmetric soliton propagates along a helical spatial line.

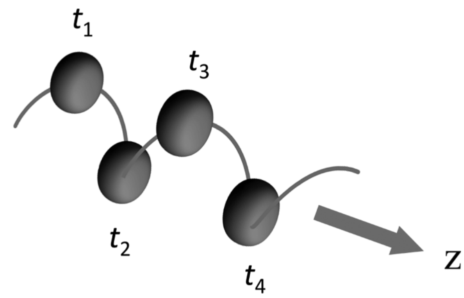

FIG. 3. Schematic representation of the dancing light bullet, which propagates in axially symmetric fiber along a spatial helical line. Designations $t_1 < t_2 < t_3 < t_4$ correspond to the different points in time t.

Instead of two equalities (16), in the axially symmetric case we have a single equality

$$\varepsilon^2 = \frac{\mu^2}{4l_D^2} + \frac{2\mathrm{sgn}(\beta_2)}{l_d l_D}. \tag{16$'$}$$

In Figs. 4 and 5 the dependencies $U(R)$ [see (26)] are displayed when the conditions (27) are carried out and when they are violated, respectively. The normal line in Fig. 4 shows the function $U(R)$ for a homogeneous bulk medium. It can be seen that in the absence of a fiber, the function $U(R)$ has a local maximum. Therefore, a stable light bullet cannot form. In the presence of a focusing fiber, a local minimum exists only if conditions (27) are satisfied. If these conditions are violated, then this local minimum disappears and the pulse undergoes irreversible self-focusing (Fig. 5).

The third inequality (27) can be rewritten in another form. From (6) it follows that the temporal amplitude ψ_m of the soliton satisfies the equality $|\psi_m|^2 = \frac{|\beta_2|}{\alpha}\rho^2$. Then for the intensity, we have $I = \frac{c}{4\pi n_0}\langle E^2\rangle = \frac{c}{2\pi n_0}|\psi_m|^2 = \frac{c}{2\pi n_0}\frac{|\beta_2|}{\alpha}\rho^2$. Here the operation $\langle\cdots\rangle$ denotes a temporal averaging. Taking into account (32) we find for peak power $P = \int_{-\infty}^{+\infty} dx \int_{-\infty}^{+\infty} I dy = \frac{c}{2n_0}\frac{|\beta_2|}{\alpha\tau_p^2}R_0^2$. Taking into account also the expressions (3) and (15), we obtain

$$P = \frac{2\pi}{n_0 n_2}\left(\frac{c}{\omega}\right)^2 \frac{l_D}{l_d} = \frac{\lambda^2}{2\pi n_0 n_2}\frac{l_D}{l_d}. \tag{34}$$

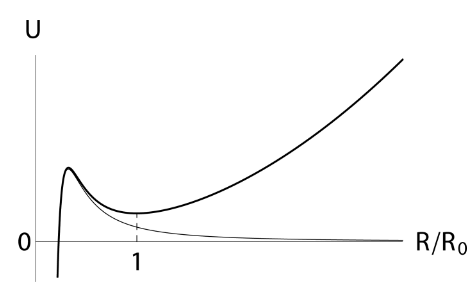

FIG. 4. Dependence of the potential energy U on the dimensionless soliton aperture R/R_0 in case of axially symmetric fiber. The bold line corresponds to the presence of fiber when the conditions (27) are satisfied. The normal line corresponds to the absence of a fiber.

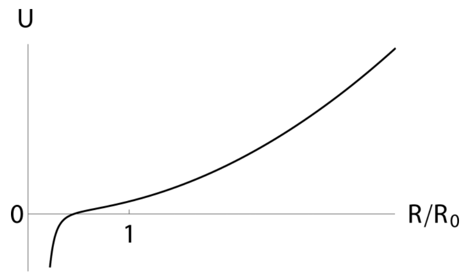

FIG. 5. Dependence of the potential energy U on the dimensionless soliton aperture R/R_0 in the presence of fiber and if at least one of the conditions (27) is violated.

From (34) it is easy to see that the third inequality (27) can be rewritten as a condition on the power of the pulse,

$$P < P_{cr}, \tag{35}$$

where the critical power

$$P_{cr} = \frac{\pi \mu^2}{6 n_0 n_2}\left(\frac{c}{\omega}\right)^2 = 0.032 \frac{\lambda^2}{n_0 n_2}. \tag{36}$$

We emphasize that the critical power defined by expression (36) differs from the critical power that is characteristic of homogeneous Kerr media [1]. In such media under the condition $P > P_{cr}$, the focusing nonlinearity prevails over the diffraction broadening. As a result, the pulse is experiencing self-focusing. If $P < P_{cr}$, the diffraction broadening suppresses self-focusing. In this case, however, the formation of a stable light bullet is impossible, because the pulse experiences an irreversible diffraction broadening (see the normal line in Fig. 4). In the fiber, under the condition (35), a stable light bullet is formed. It is important to note that the power in inequality (35) is not the input power of the pulse, but the power of the formed spatiotemporal soliton.

Assuming in (17) and (18) $q_{j0} = 0$, we have, in conjunction with (6), a solution in the form of a light bullet propagating parallel to the axis of the fiber. Following [22], we call this bullet a fundamental spatiotemporal soliton. The expressions (31) and (32) under the condition $\mathbf{r}_c = 0$ correspond to the axially symmetric fundamental soliton (Fig. 6).

It is important to note that in (16), (21)–(23), and also in (16′), (27)–(30), (35), and (36), there are no parameters q_{j0} and $\mathbf{r}_c$. That is, the stability conditions are the same for both the dancing light bullet and the fundamental soliton. These conditions do not depend on the trajectory along which the spatiotemporal soliton propagates.

We present some numerical estimates. Let the optical fiber be made of fused silica. In the near-infrared range for $\lambda = 1.55\,\mu$m we have $n_0 \approx 1.5$, $\beta_2 = -2.0 \times 10^{-28}$ s^2/cm,

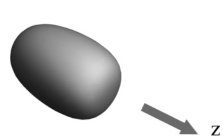

FIG. 6. Schematic representation of a constant-intensity surface of the fundamental spatiotemporal soliton in an axially symmetric fiber.

and $n_2 = 3.2 \times 10^{-16}$ cm^2/W [6]. Putting $a \sim 0.1$ cm, from (28) and (29) we find $R_{\min} \sim 10\,\mu$m, $\tau_{\min} \sim 10^{-14}$ s. Let $R_0 \sim 100\,\mu$m and $\tau_p \sim 1$ ps. Then we have $l_D = 2\pi n_0 R_0^2/\lambda \sim 1$ cm, $l_d \sim 10^4$ cm. From (36) and (34) we find $P_{cr} \sim 10^6$ W, $P \sim 10^3$ W $\ll P_{cr}$.

Thus, here the diffraction limit condition (A9) is satisfied with a good margin. This condition can also be written as $P \ll P_{cr}$.

The parameters chosen above are typical for nonresonant optical pulses and fused silica fibers. At the same time, with the shortening of the duration of the light pulse, it becomes more difficult to satisfy conditions (29) and (30). In addition, the parameters of the fiber may vary. This relates, for example, to the parameters β_2 and a. In this regard, the conditions (27) and (28)–(30) are very important for the formation of a stable light bullet in a focusing fiber.

IV. DIFFRACTION LIMIT

The numerical estimates given at the end of the previous section correspond to the diffraction limit: $P \ll P_{cr}$ or $l_D/l_d \ll \mu^2/12$. In this case, in the formulas describing the transverse dynamics of the pulse, we can formally consider $l_d \to \infty$. Then the stability conditions (27) are automatically satisfied.

In this section, we restrict ourselves to the consideration of an axially symmetric fiber. The generalization to the case of an anisotropic fiber is obvious and not difficult.

From (16′) in the limit $l_d \to \infty$ for the axially symmetric case we have $l_D = \frac{\mu}{2\varepsilon}$. That is, the soliton aperture is uniquely determined by the parameter a of the fiber:

$$R_0 = \left(\frac{\mu}{4\pi\sqrt{n_0^2 - 1}}\right)^{1/2} \sqrt{\lambda a} \approx 0.35 \frac{\sqrt{\lambda a}}{\left(n_0^2 - 1\right)^{1/4}}. \tag{37}$$

The expression (37) is in agreement with inequality (28). It is easy to see that the aperture defined by expression (37) corresponds to the first transverse mode of the optical fiber. In the diffraction limit, the transverse dynamics of a soliton is practically independent of its longitudinal dynamics. Therefore, in the theoretical description of the propagation of a pulse in an optical fiber, a factorized representation $\psi(z, \mathbf{r}, \tau) = \Psi(z, \tau)\Sigma(\mathbf{r})$ is often used [1,6]. After averaging Eq. (1) over the transverse coordinates for the function $\Psi(z, \tau)$, the one-dimensional nonlinear Schrödinger equation is derived [1,6].

Under the condition $l_d \to \infty$, the formulas (16′), (31), and (32) correspond to the nonstationary coherent state of a two-dimensional quantum harmonic oscillator. The corresponding solution can be obtained from (12) with $\beta_2 = 0$ and by taking into account (2) and (13), by means of the well-known Green's function for the harmonic oscillator [23].

A large number of other solutions of the linear Schrödinger equation are known [24]. Using these solutions, one can describe various modes of propagation of light bullets corresponding to the diffraction limit. For example, in the case of an axially symmetric fiber, we write the solution for the stationary state of a two-dimensional quantum harmonic oscillator,

$$\Phi_{m_x,m_y}(x,y,z) = \frac{1}{\sqrt{\tau_p}} H_{m_x}\left(\frac{x}{R_0}\right) H_{m_y}\left(\frac{y}{R_0}\right) \exp\left(-i w_{m_x,m_y} z\right) \times \exp\left(-\frac{x^2+y^2}{4R_0^2}\right), \quad (38)$$

where H_{m_j} are the Hermite polynomials,

$$w_{m_x,m_y} = \varepsilon(m_x+m_y+1) = \frac{\sqrt{n_0^2-1}}{n_0 a}(m_x+m_y+1), \quad (39)$$

where $m_x, m_y = 0, 1, 2, \cdots$; aperture R_0 is defined by the expression (37).

Because Eq. (12) under the condition $\beta_2 = 0$ is linear, then in accordance with the principle of superposition we write

$$\Phi(x,y,z) = \sum_{m_x,m_y} C_{m_x,m_y} \Phi_{m_x,m_y}(x,y,z), \quad (40)$$

where C_{m_x,m_y} are the dimensionless complex constants determined by the conditions at the input to the fiber.

The case when all the constants C_{m_x,m_y} are zero, except $C_{0,0}$, corresponds to the fundamental soliton under the condition $P \ll P_{cr}$.

Putting

$$C_{m_x,m_y} = \frac{1}{m_x! m_y!}\left(\frac{iq_0}{2R_0}e^{-i\delta_x}\right)^{m_x}\left(\frac{iq_0}{2R_0}e^{-i\delta_y}\right)^{m_y} \times \exp\left(-\frac{q_0^2}{4R_0^2}\right), \quad (41)$$

where R_0 is defined by the expression (37), $\delta_{x,y}$ and q_0 are the constants, we have a coherent state of a two-dimensional quantum harmonic oscillator described by Eq. (12) under the condition $\beta_2 = 0$. It is easy to see that this state corresponds to the axially symmetric dancing light bullet considered above in the diffraction limit ($l_d \to \infty$).

Let $C_{1,0} = 1$, and all others, C_{m_x,m_y}, be zero. Then from (38), (39), and (11) we have

$$\rho = \frac{x^2}{2\tau_p R_0^2}\exp\left(-\frac{x^2+y^2}{2R_0^2}\right), \quad \theta = 2\mu\frac{\sqrt{n_0^2-1}}{n_0 a}z.$$

This solution coincides qualitatively with the stationary version of the two-mode (dipole) solution found in [22]. However, the dipole solution obtained in [22] is more general, since it goes beyond the diffraction limit.

Now suppose that on the input to the fiber we have a coherent superposition (40) of the fundamental soliton (only $C_{0,0} \neq 0$, Fig. 6) and the quadrupole soliton mode of the fiber (only $C_{1,1} \neq 0$, Fig. 7). In this case, we have

$$\rho = \frac{1}{\tau_p}\left[C_{00}^2 + \frac{C_{11}^2}{4R_0^4}x^2y^2 + \frac{C_{00}C_{11}}{R_0^2}xy\cos(2\varepsilon z)\right]\exp\left(-\frac{x^2+y^2}{2R_0^2}\right). \quad (42)$$

As can be seen from (6) and (42), in the process of propagation, the shape of such a spatiotemporal soliton periodically repeats with a spatial period $\pi/\varepsilon = \pi n_0 a/\sqrt{n_0^2-1}$ (see Fig. 8). This phenomenon is called the self-imaging effect in a multimode fiber [25–27]. In our case, we have described the soliton version of the self-imaging effect. Of course, it is possible to take a superposition of a much larger quantity of modes than in the considered example. Then the self-imaging effect will manifest itself in the form of spatial beats of a large number of the fiber modes. On the other hand, the problem of the realization of such superposition states under experimental conditions seems to be difficult. On the other hand, any spatiotemporal signal can be approximately represented as an expansion on the finite number of spatial modes of the fiber. Then, as a result of the interference of these modes, it will be possible to observe the self-imaging effect.

In the same way, solutions like localized vortices, entangled states [28–30], etc., can be constructed and analyzed.

In the diffraction limit, it is easy to obtain a condition in which the pulse is trapped by the focusing fiber. At the boundary of an axially symmetric fiber, we have $r = a$. Then the depth V of the potential well in Eq. (12) under the condition $\beta_2 = 0$ is determined by the expression $V = |g/\mu|_{r=a}$. To form a stationary state $\Phi_{m_x,m_y}(x,y,z)$, the condition $V > w_{m_x,m_y}$ must be satisfied. Using here (2), (10), (13), (24), and

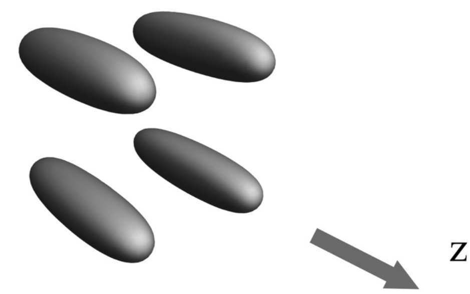

FIG. 7. Schematic representation of constant-intensity surfaces of a soliton quadrupole fiber mode.

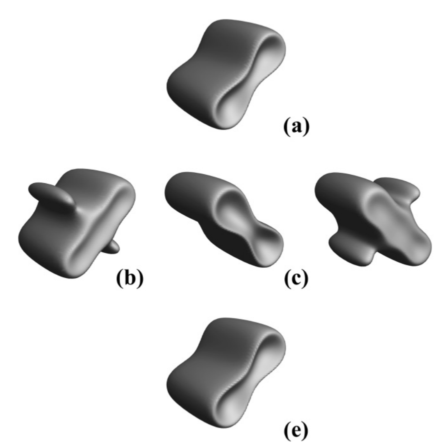

FIG. 8. Schematic illustration of soliton version of the self-imaging effect. The light bullet is formed by a coherent superposition of the fundamental soliton and the quadrupole spatiotemporal mode of the fiber. Images (a–e) correspond to successive changes in the shape of a light bullet when propagating in a fiber. Images (a) and (e) are identical. That is, the light bullet periodically restores its spatiotemporal profile.

(39), we rewrite this condition as

$$\frac{a}{\lambda}\sqrt{n_0^2-1} > 0.5(m_x+m_y+1). \quad (43)$$

Assuming here $m_x = m_y = 0$, we find for a fundamental soliton $\frac{a}{\lambda}\sqrt{n_0^2-1} > 0.5$. For the dipole ($m_x = 1, m_y = 0$) and quadrupole ($m_x = m_y = 1$) solitons we have $\frac{a}{\lambda}\sqrt{n_0^2-1} > 1$ and $\frac{a}{\lambda}\sqrt{n_0^2-1} > 1.5$, respectively. With the parameters given at the end of the previous section, these conditions are well satisfied.

The dancing light bullet is a superposition (40), where m_x and m_y lie in the interval from zero to infinity. It is clear that for very large m_x and m_y the condition (43) is not satisfied. Then, in order to trap a dancing light bullet into the fiber, it is necessary that the contribution of stationary states with large values of m_x and m_y should be insignificant. From (41) it can be seen that the absolute values of the coefficients C_{m_x,m_y} are decreased with the increasing of m_x and m_y, if the condition $q_0 < 2\sqrt{2}R_0 \approx 2.83R_0$ is satisfied. Thus, the center of the dancing light bullet should not deviate too far from the axis of the fiber. This condition is consistent with the paraxial approximation.

Since in the diffraction limit the conditions (27) [see also (28)–(30) and (35)] are performed with a good margin, in this limit the transverse soliton dynamics is insensitive to Kerr nonlinearity and group velocity dispersion. In this case, however, the signs of the Kerr nonlinearity and the dispersion of the group velocity are very important for the formation of a soliton in the direction of its propagation. This once again confirms the conclusion that under the conditions of the diffraction limit, the longitudinal and transverse dynamics of the light pulse are independent of each other.

The question arises of how a dancing light bullet can be created under experimental conditions. To do this, you first need to create a laser bunch of light energy, exponentially localized in all directions. Then, this bunch should be directed into the fiber at a certain small angle $\sim q_{x,y}/a_{x,y}$ with respect to axis of this fiber. At the same time, it is highly desirable that the parameters of this bunch be connected by the equalities (16) [or (16′)] and satisfy the conditions (21)–(23). This is most easily seen in the case of an axially symmetric fiber. In this case, the conditions (21)–(23) take the form of inequalities (28)–(30). In the diffraction limit, conditions (29) and (30) are automatically satisfied. At the same time, the aperture of the laser bunch directed into the fiber should be close to the value determined by formula (37). In this case, one can hope that a dancing light bullet will be formed in the fiber. If the laser bunch is directed into the fiber along its axis, then there is reason to believe that in the fiber it will be transformed into a fundamental spatiotemporal soliton.

In fibers, the temporal solitons are usually observed. Apparently this is due to the fact that the transverse structure eludes observation. In the diffraction limit the transverse structure of solitons is determined by the spatial eigenmodes of the fiber.

The light bullets discussed here, including the soliton effect of self-imaging, can find applications in information transmission and coding systems.

V. CONCLUSION

Thus, on the basis of the averaged Lagrangian method, one can describe the propagation of a wide class of spatiotemporal solitons in optical fibers.

The dancing light bullet, described by expressions (6), (17), and (18), has been studied in most detail here. The parameters q_{10} and q_{20} have the meaning of the amplitudes of the deviation of the center of the bullet from the fiber axis along the x and y axes, respectively. Under the conditions $q_{x0} = q_{y0} = 0$ the dancing light bullet transforms into a fundamental spatiotemporal soliton, propagating along the fiber axis with a constant group velocity.

It is important to note that the stability conditions (21)–(23) look the same for a dancing light bullet and for a fundamental spatiotemporal soliton. This is due to the nontrivial result that the dynamics of the transverse coordinates q_x and q_y of the center of the light bullet does not depend on the dynamics of its aperture. If the fiber and the light bullet are axially symmetric, the stability conditions (21)–(23) have the most visual meaning, taking the form of restrictions (28)–(30) for the aperture R_0 and temporal duration τ_p. In this case, the condition (30) can be written in the form of a restriction (35) for the power P of the light bullet, where the critical power P_{cr} is determined by expression (36).

In the diffraction limit $P \ll P_{cr}$, the transverse and longitudinal dynamics of the light bullet are practically independent of each other. In this case the transverse dynamics is described by Eq. (12) under the condition $\beta_2 = 0$. At the same time, let us note that in the expression (6) $\beta_2 \neq 0$. In this case Eq. (12) coincides with the linear quantum-mechanical Schrödinger equation for a particle in a two-dimensional potential well. This greatly facilitates the analysis of the transverse structure and dynamics of the spatiotemporal soliton. The role of the potential here belongs to the coefficient $g(\mathbf{r})/\mu$ characterizing the spatial distribution of the refractive index over the cross section of the graded-index fiber. In this case we can use profiles of $g(\mathbf{r}) \sim f(\mathbf{r})$ [see (2)], which differ from the parabolic profile (13).

In this paper, we described the soliton self-image effect in the diffraction limit $P \ll P_{cr}$. It is of interest to study this effect in a more general case. For this, it is necessary to find multimode solutions of Eq. (12) under the condition $\beta_2 \neq 0$.

It is clear that the parabolic dependence of the refractive index on x and y is valid only near the axis of the fiber. Approaches are known for obtaining nonstationary solutions of the quantum-mechanical Schrödinger equation in the case of different profiles of $g(\mathbf{r})/\mu$ [24]. This includes refractive index profiles that are close to real profiles.

Here we used the averaged Lagrangian method for Eq. (1). It does not take into account the dependence of the nonlinear refractive index n_2 on $\mathbf{r}$. However, by means of the approach used here, this can be done. There are no principal difficulties this way.

Equation (1) can be used for pulses whose duration satisfies the condition $\tau_p \geqslant 100$ fs. If $\tau_p \sim 10$ fs, then Eq. (1) must be supplemented with higher orders of linear and nonlinear dispersion [1,6]. It is desirable to develop the averaged Lagrangian method for these cases.

It is also of interest to develop this approach to study the propagation of an optical pulse in a system of coupled parallel optical fibers. The consideration of few-cycle spatiotemporal solitons [31,32] deserves special attention here. In this case, one cannot use the approach of slowly varying envelopes.

It is known that in homogeneous media under the condition $P \gg P_{cr}$ the small-scale self-focusing modes can be implemented, followed by the filamentation of optical pulses [33,34]. It is of interest to generalize the averaged Lagrangian approach for describing a small-scale self-focusing of pulses in the fiber.

Of considerable interest is the study of the mutual interaction of spatiotemporal solitons in fibers. Here we can talk, for example, about the interaction of the polarization components of a pulse in a birefringent fiber [35,36]. In this case, instead of one Eq. (1), we must write the system of two nonlinear equations for the envelopes of the ordinary ψ_o and extraordinary ψ_e pulse components. In addition to the Kerr nonlinearity composed of ψ_o and ψ_e, these equations contain waveguide terms $g_o(\mathbf{r})\psi_o$ and $g_e(\mathbf{r})\psi_e$. To use the averaged Lagrangian method here, it is necessary to choose trial solutions correctly. For this, in turn, it is desirable to have exact solutions of the original nonlinear system of equations in the form of one-dimensional (temporal) solitons. After this, there should be no fundamental difficulties.

ACKNOWLEDGMENTS

The author thanks Prof. A. I. Maimistov, Dr. A. N. Bugay, and Dr. V. A. Khalyapin for the helpful discussions. This work was carried out with the financial support of the Russian Science Foundation (Project No. 17-11-01157).

APPENDIX

Generalizing the results of works [11,13,18,20], we find a solution of system (8) and (9) in the following form:

$$\rho = \frac{1}{\tau_p}\frac{R_{x0}R_{y0}}{R_xR_y}F(\xi,\eta), \tag{A1}$$

$$\varphi = \alpha + \sigma_x x + \gamma_x\frac{x^2}{2} + \sigma_y y + \gamma_y\frac{y^2}{2}, \tag{A2}$$

where τ_p, R_{x0}, and R_{y0} are the constants; F is the dimensionless unknown function of variables;

$$\xi = \frac{x-q_x}{R_x}, \quad \eta = \frac{y-q_y}{R_y}, \tag{A3}$$

and $R_{x,y}(z)$, $q_{x,y}(z)$, $\alpha(z)$, $\sigma_{x,y}(z)$, and $\gamma_{x,y}(z)$ are the unknown functions of the z coordinate.

The parameter τ_p has the meaning of the equilibrium temporal duration of the spatiotemporal soliton [see (5) and (6)]. At the same time, through the parameters R_{j0} the diffraction scale lengths l_{Dj} are determined [see (15)].

The coefficient $\alpha(z)$ determines a nonlinear part of the refractive index, the coefficients $\sigma_{x,y}(z)$ determine the rotation of the wave fronts with respect to the direction of propagation of the pulse, and the coefficients $\gamma_{x,y}(z)$ determine the curvature of the wave fronts.

Near the local maximum of the soliton profile, we have $F \sim 1$. On the other hand, in order for the soliton energy to be finite, it is necessary to satisfy the condition $F(\xi,\eta) \to 0$ at $\sqrt{\xi^2+\eta^2} \to \infty$.

Substituting (A1) and (A2) into (8) with accounting for (A3), we obtain

$$\frac{1}{R_xR_y}\left(\gamma_x - \frac{R_x'}{R_x} + \gamma_y - \frac{R_y'}{R_y}\right)F + \frac{1}{R_x^2R_y}\left[\sigma_x - q_x' + \frac{R_x'}{R_x}q_x + \left(\gamma_x - \frac{R_x'}{R_x}\right)x\right]\frac{\partial F}{\partial \xi} + \frac{1}{R_xR_y^2}\left[\sigma_y - q_y' + \frac{R_y'}{R_y}q_y + \left(\gamma_y - \frac{R_y'}{R_y}\right)y\right]\frac{\partial F}{\partial \eta} = 0,$$

where the prime above denotes the derivative with respect to z.

From here we set

$$\gamma_j = \frac{R_j'}{R_j}, \tag{A4}$$

$$\sigma_j = q_j' - \frac{R_j'}{R_j}q_j. \tag{A5}$$

Substituting (A1) and (A2) into (9), and taking into account (2), (13), (A3), and (A4), we obtain

$$\alpha' + \frac{1}{2}(\sigma_x^2+\sigma_y^2) + \left(\sigma_x' + \frac{R_x'}{R_x}\sigma_x\right)x + \left(\sigma_y' + \frac{R_y'}{R_y}\sigma_y\right)y + \left(\frac{R_x'}{R_x} + \varepsilon_x^2\right)\frac{x^2}{2} + \left(\frac{R_y'}{R_y} + \varepsilon_y^2\right)\frac{y^2}{2} + \frac{c\beta_2}{2n_0\omega\tau_p^2}\frac{R_{x0}^2R_{y0}^2}{R_x^2R_y^2}F^2 = \frac{\mu^2}{2}\left(\frac{c}{n_0\omega}\right)^2\frac{1}{\sqrt{F}}\left(\frac{1}{R_x^2}\frac{\partial^2\sqrt{F}}{\partial\xi^2} + \frac{1}{R_y^2}\frac{\partial^2\sqrt{F}}{\partial\eta^2}\right). \tag{A6}$$

Now we need to find the function $F(\xi,\eta)$. The ratio of the last term on the left-hand side of Eq. (9) to the right-hand side of this equation is on an the order of magnitude equal to $\sim l_{Dj}/l_d$.

To obtain an exact solution, the third term on the left-hand side of (9) and the right-hand side of this equation must be second-degree polynomials with respect to the variables x and y. At the same time, the function F must be localized on these variables.

In the approximation of geometrical optics,

$$l_{Dj}/l_d \gg 1 \tag{A7}$$

should be neglected from the term on the right-hand side of (9), $\sim\mu^2\Delta_\perp\sqrt{\rho}/\sqrt{\rho}$. Then, putting F in the form

$$F(\xi,\eta) = \sqrt{1-(\xi^2+\eta^2)}, \tag{A8}$$

we have the exact solution of system (8) and (9) under the formal condition $\mu = 0$.

Obviously, the condition $\xi^2+\eta^2 \leqslant 1$. If $\xi^2+\eta^2 > 1$, then we have $F = 0$.

Now let the diffraction limit condition be satisfied:

$$l_{Dj}/l_d \ll 1. \tag{A9}$$

In this case we can neglect the third term $\frac{c\beta_2}{2n_0\omega}\rho^2$ on the left-hand side of (9).

Then at

$$F(\xi,\eta)=\exp\left(-\frac{\xi^2+\eta^2}{2}\right), \quad (A10)$$

the right-hand side of Eq. (A6) will be a polynomial of second degree with respect to the variables x and y.

Thus, under opposite limits (A7) and (A9) we can assume formally in (9) $\mu=0$ and $\beta_2=0$, respectively. In these limits the exact solutions of system (8) and (9) can be found. Now we find an approximate solution that is valid under both conditions (A7) and (A9) and in the intermediate case. To do this, we note that the right-hand sides of (A8) and (A10) transform into each other, if $\xi^2+\eta^2\ll 1$:

$$F(\xi,\eta)\approx 1-\frac{\xi^2+\eta^2}{2}. \quad (A11)$$

It is this vicinity near the maximum of the function $F(\xi,\eta)$ that has the most significant effect on the dynamics [11,13,18,20].

Taking this into account, we approximately consider the expression (A10) to be fair, using the expansion (A11) in the third term of the left-hand side of Eq. (9).

Let us note that such an approximate approach agrees well with numerical simulations in solving other similar problems [12,20].

Then, equating to each other the coefficients at various degrees and on the left- and right-hand sides of Eq. (9), we obtain the set of equations

$$\alpha'=-\frac{1}{2}\sum_{j=x,y}\left[\sigma_j^2+\left(\frac{\mu c}{n_0\omega}\right)^2\frac{1}{2R_j^2}\left(1-\frac{q_j^2}{2R_j^2}\right)\right]$$
$$-\frac{\mathrm{sgn}(\beta_2)}{l_d}\frac{c}{n_0\omega}\frac{R_{x0}^2R_{y0}^2}{R_x^2R_y^2}\left(1-\sum_{j=x,y}\frac{q_j^2}{R_j^2}\right), \quad (A12)$$

$$\sigma'_{x,y}+\frac{R'_{x,y}}{R_{x,y}}\sigma_{x,y}=-\frac{c}{n_0\omega}\left[\frac{\mu^2}{4}\frac{c}{n_0\omega}\frac{1}{R_{x,y}^4}+\frac{\mathrm{sgn}(\beta_2)}{l_d}\frac{R_{x0}^2R_{y0}^2}{R_{x,y}^4R_{y,x}^2}\right]q_{x,y}, \quad (A13)$$

$$R''_{x,y}=-\frac{\partial U}{\partial R_{x,y}}, \quad (A14)$$

$$U(R_x,R_y)=\frac{\varepsilon_x^2}{2}R_y^2+\frac{\varepsilon_x^2}{2}R_y^2+\frac{\mu^2}{8}\left(\frac{c}{n_0\omega}\right)^2\left(\frac{1}{R_x^2}+\frac{1}{R_y^2}\right)$$
$$+\frac{c}{n_0\omega}\frac{\mathrm{sgn}(\beta_2)}{l_d}\frac{R_{x0}^2R_{y0}^2}{R_x^2R_y^2}. \quad (A15)$$

As a result, we have a self-consistent system of Eqs. (A4), (A5), and (A12)–(A15) for the dynamic parameters, which are introduced in (A1)–(A3).

Differentiating (A5) with respect to z, we obtain

$$q'_j=\left(\frac{R'_j}{R_j}-\frac{R'^2_j}{R_j^2}\right)q_j+\sigma'_j+\frac{R'_j}{R_j}q'_j$$
$$=\left(\frac{R'_j}{R_j}-\frac{R'^2_j}{R_j^2}\right)q_j+\sigma_j+\frac{R'_j}{R_j}\left(\frac{R'_j}{R_j}q_j+\sigma_j\right)$$
$$=\frac{R'_j}{R_j}q_j+\sigma'_j+\frac{R'_j}{R_j}\sigma_j.$$

Using now (A13)–(A15), we have

$$q''_j=-\varepsilon_j^2q_j. \quad (A16)$$

Thus, the dynamic variables q_j describing the motion of the soliton center obey the harmonic oscillator equation (A16). It is important that these variables do not depend on the dynamics of the soliton apertures $R_{x,y}(z)$.

From (A16) we find

$$q_j=q_{j0}\sin(\varepsilon_jz+\delta_j), \quad (A17)$$

where q_{j0} and δ_j are the amplitudes and phase shifts, respectively.

[1] Yu. S. Kivshar and G. P. Agrawal, *Optical Solitons: From Fibers to Photonic Crystals* (Academic Press, New York, 2003).
[2] H. Zhang, D. Tang, L. Zhao, Q. Bao, and K. P. Loh, Opt. Commun. **283**, 3334 (2010).
[3] H. Zhang, D. Y. Tang, L. M. Zhao, and R. J. Knize, Opt. Express **18**, 4428 (2010).
[4] H. Zhang, D. Y. Tang, L. M. Zhao, and X. Wu, Phys. Rev. B **80**, 052302 (2009).
[5] N. Akhmediev, J. M. Soto-Crespo, and G. Town, Phys. Rev. E **63**, 056602 (2001).
[6] G. P. Agrawal, *Nonlinear Fiber Optics* (Academic Press, Boston, 1989).
[7] D. Anderson, Phys. Rev. A **27**, 3135 (1983).
[8] S. K. Zhdanov and B. A. Trubnikov, Zh. Eksp. Teor. Fiz. **92**, 1612 (1987) [Sov. Phys. JETP **65**, 904 (1987)].
[9] S. K. Zhdanov and B. A. Trubnikov, *Quasi-gaseous Unstable Media* (Nauka, Moscow, 1991).
[10] D. Anderson, M. Desaix, M. Lisak, and M. L. Quorida-Teixeiro, J. Opt. Soc. Am. B **9**, 1358 (1992).
[11] S. V. Sazonov, JETP **103**, 126 (2006).
[12] A. N. Bugay and S. V. Sazonov, Phys. Rev. E **74**, 066608 (2006).
[13] S. V. Sazonov, J. Phys. Soc. Jpn. **85**, 124404 (2016).
[14] S. S. Yu, C. H. Chien, Y. Lai, and J. Wang, Opt. Commun. **119**, 167 (1995).
[15] S. Raghavan and G. P. Agrawal, Opt. Commun. **180**, 377 (2000).
[16] D. R. Tilley and J. Tilley, *Superfluidity and Superconductivity* (Van Nostrand Reinhold, New York, 1974).
[17] H. Lamb, *Hydrodynamics*, 6th ed. (Cambridge University Press, Cambridge, 1994).
[18] S. A. Akhmanov, A. P. Sukhorukov, and R. V. Khokhlov, Sov. Phys. Usp. **10**, 609 (1968).
[19] C. Rogers and B. Malomed, J. Math. Phys. **59**, 051506 (2018).

[20] S. V. Sazonov, M. S. Mamaikin, M. V. Komissarova, and I. G. Zakharova, Phys. Rev. E **96**, 022208 (2017).
[21] F. Dalfovo, S. Giorgini, L. P. Pitaevskii, and S. Stringari, Rev. Mod. Phys. **71**, 463 (1999).
[22] O. V. Shtyrina, M. P. Fedoruk, Yu. S. Kivshar, and S. K. Turitsyn, Phys. Rev. A **97**, 013841 (2018).
[23] M. O. Scully and M. S. Zubairy, *Quantum Optics* (Cambridge University Press, Cambridge, 1997).
[24] S. Flügge, *Practical Quantum Mechanics* (Springer-Verlag, Berlin, 1971), Vol. 1.
[25] G. P. Agrawal, A. K. Chatak, and C. I. Mehta, Opt. Commun. **12**, 333 (1974).
[26] L. Jacomme, Appl. Opt. **14**, 2578 (1975).
[27] G. P. Agrawal, Opt. Fiber Technol. **50**, 309 (2019).
[28] M. V. Berry, J. Opt. A **6**, 259 (2004).
[29] J. Leach, E. Yao, and M. J. Padgett, New J. Phys. **6**, 71 (2004).
[30] G.-L. Oppo, A. J. Scroggie, and W. J. Firth, Phys. Rev. E **63**, 066209 (2001).
[31] S. Terniche, H. Leblond, D. Mihalache, and A. Kellou, Phys. Rev. A **94**, 063836 (2016).
[32] H. Leblond and D. Mihalache, J. Phys. A: Math. Theor. **51**, 435202 (2018).
[33] R. W. Boyd, S. G. Lukishova, and Y. R. Shen, *Self-focusing: Past and Present* (Springer, New York, 2009).
[34] S. V. Chekalin and V. P. Kandidov, Phys. Usp. **56**, 123 (2013).
[35] H. Zhang, D. Y. Tang, L. M. Zhao, and N. Xiang, Opt. Express **16**, 12618 (2008).
[36] H. Zhang, D. Y. Tang, L. M. Zhao, and H. Y. Tam, Opt. Lett. **33**, 2317 (2008).